Introducing a Partitioning Mechanism for PAHs into the Community Multiscale Air Quality Modeling System and Its Application to Simulating the Transport of Benzo(a)pyrene over Europe

ARMIN AULINGER, VOLKER MATTHIAS, AND MARKUS QUANTE

GKSS Research Centre, Institute for Coastal Research, Geesthacht, Germany

(Manuscript received 19 January 2006, in final form 10 January 2007)

ABSTRACT

Into the Community Multiscale Air Quality modeling system (CMAQ) that is widely used for simulating the transport and fate of air pollutants, a new module was inserted that accounts for the partitioning of semivolatile organic compounds—in particular, polycyclic organic hydrocarbons (PAHs)—between the gaseous and the particulate phases. This PAH version of CMAQ can at this time be applied to substances that are predominantly associated with particles and can be assumed to be inert, as is the case for benzo(a)pyrene [B(a)P]. The model was set up for Europe on a grid with 54-km cell width with a nest of 18-km gridcell width located around the North Sea to simulate ambient air concentrations and depositions of B(a)P in January, April, July, and October 2000. To evaluate the quality of the simulation results, daily and monthly mean concentrations were compared with measurements from six monitoring stations. The typical ratio of modeled to measured values is circa 4 (median), which—with respect to both measurement and simulation uncertainties and problems involved when comparing measurements with simulations—proved that the PAH version of CMAQ is suitable to simulate the fate and transport of B(a)P over Europe and can serve as a starting point for models for other PAHs that additionally consider degradation.

1. Introduction

Polycyclic organic hydrocarbons (PAHs) belong to the so-called persistent organic pollutants (POPs), a group of substances with known adverse effects on ecosystems and human health. Single ones or mixtures of these compounds can, for example, cause cancer or impair reproduction (Mumatz and George 1995). The concentrations of PAHs in the environment are relatively low, but they gain their extraordinary ecotoxicity from their persistency in various environmental compartments (atmosphere, soil, water, biota) in conjunction with a high bioaccumulative potential and lifelong exposure of individuals. This has been confirmed in various studies in which PAHs and other POPs were measured in fish, marine mammals, seabirds, and humans (Baussant et al. 2001; MacDonald et al. 2000). In conclusion, several international conventions were initiated to reduce or phase out the most hazardous of these substances; examples include the United Nations Economic Commission for Europe (UN-ECE) POP Protocol, the Oslo and Paris Commission (OSPAR) and the Helsinki Commission (HELCOM) conventions for the North Atlantic and the Baltic Sea, the United States–Canadian Great Lakes Water Quality Agreement, and the Stockholm convention released in May 2004 by the United Nations Environment Program (UNEP). These conventions have raised an interest in relating spatial and temporal information on the release of POPs into the environment (i.e., the emissions) with the risk posed by their presence in particular environments. The rationale is that if such a quantitative relationship can be established then the most efficient means of reducing the risk by reducing emissions can be sought. This approach is essentially the one adopted in response to the UN-ECE protocol on POPs. An important part of this approach is the use of numerical simulation models of the atmospheric transport of POPs both on a regional European scale and on a global scale.

PAHs are semivolatile compounds that can be transported in the atmosphere over large distances either as gaseous species or while bound to fine particles. They

Corresponding author address: Armin Aulinger, GKSS Research Centre, Institute for Coastal Research, Max-Planck-Str. 1, Geesthacht D-21502, Germany.
E-mail: armin.aulinger@gkss.de

DOI: 10.1175/2007JAMC1395.1

are mainly generated by incomplete combustion of organic matter. Small amounts are also present in crude oil and engine fuels. Almost all of the sources are anthropogenic—for example, road transport, energy production, and waste incineration (Wild and Jones 1995). Their lifetime in the atmosphere depends on their vapor pressure, their affinity to water and organic solvents, and their resistance to photolytic and photochemical degradation. To simulate adequately the processes that determine the transport, degradation, and deposition of PAHs and other POPs, it is essential to have a chemical transport model that represents the state-of-the-art in atmospheric modeling as well as in aerosol chemistry and dynamics.

Only a few modeling techniques have been developed for exploration of atmospheric processes of POPs. These include relatively simple mass balance models that examine the pooling and exchange of POPs between various environmental compartments (Wania and Mackay 1999), as well as recently developed deterministic atmospheric dispersion models incorporating a more detailed treatment of physical and chemical atmospheric processes of POPs (Shatalov et al. 2000; Gusev et al. 2005). Some of these models use advanced chemical schemes for POPs but simple meteorological parameterizations or they can only use a coarse model domain resolution. A model intercomparison study initiated by the Meteorological Synthesizing Center East (MSCE) was still in process at the time of writing (Shatalov et al. 2004).

In this contribution, an extension to the Community Multiscale Air Quality modeling system (CMAQ) is presented that enables one to use the model to quantify the atmospheric transport and deposition of PAHs over Europe. The basic version of CAMQ 4.5 is modified to read the emissions and to simulate the transport, scavenging, and deposition of PAHs either adsorbed to particles discerned into three modes or as gaseous molecules. The first model runs have been carried out for January, April, July, and October of 2000, with benzo(a)pyrene [B(a)P] as an example PAH.

The CMAQ-B(a)P model described here is considered to be an important step toward using comprehensive Eulerian model frameworks for the assessment of atmospheric pathways of transport, transformations, and deposition of PAHs and other POPs on their way from emissions to deposition over spatial scales from about a hundred kilometers to continental.

2. Model approach

CMAQ is a 3D Eulerian regional model, which is in our case geographically adapted to the European continent. The entire model domain covers Europe from the Mediterranean Sea to the North Polar Sea and from Iceland to western Russia, with a gridcell size of 54 km $\times$ 54 km. A second domain placed around the North Sea coast from the Netherlands to Denmark with a cell size of 18 km $\times$ 18 km was nested into the large domain. Because boundary layer processes play a dominant role in vertical and horizontal transport of atmospheric pollutants, especially in coastal regions, the high number of 30 vertical levels, including 18 levels below 2000 m, has been chosen. The grid with 18-km horizontal grid spacing is a compromise between a reasonable resolution and limited computing power, having in mind the long-term runs (several years) for which we are aiming. Local convective phenomena call for a grid resolution of a few kilometers or better. Sea breezes can probably not be adequately modeled with the 18-km spacing, although they may develop as simulations with 36-km grid spacing indicate (Colby 2004). Our primary area of interest is the North Sea coast, with focus on the German bight. This coastline is considerably less complex than those investigated by the studies calling for high grid resolution. Further, we assume that the unresolved flow features are not changing long-term statistics of pollutant concentration and deposition over larger areas in a relevant manner.

The input meteorological fields were computed with the fifth-generation Pennsylvania State University–National Center for Atmospheric Research (NCAR) Mesoscale Model (MM5) (Grell et al. 1995) using sophisticated algorithms for the representation of cloud microphysics [Reisner scheme, including graupel (Reisner et al. 1998)], subgrid cloud parameterization [Kain–Fritsch-2 scheme, including shallow convection (Kain and Fritsch 1993; Kain 2004)], planetary boundary layer processes [Medium Range Forecast (MRF) Model scheme based on Hong and Pan (1996)], and radiation (considering cloud effects on radiation). Last, the Meteorology–Chemistry Interface Preprocessor (MCIP), version 3.0, (Otte 1999) was used to calculate the required meteorological variables from the meteorological fields to drive the CMAQ Chemistry Transport Model (CCTM).

The Carbon Bond 4 (CB4) chemical mechanism (Gery et al. 1989), including aerosol and aqueous phase chemistry, was used to account for the reactions and formations of trace gases and particles. In version 4.5 of CMAQ, which was used in this study, aerosols are divided into three modes according to their diameter (Binkowski and Shankar 1995). The Aitken mode includes particles with diameters of less than 0.1 μm, the accumulation mode covers diameters between 0.1 and 2.5 μm, and the coarse mode takes into account par-

ticles with diameters between 2.5 and 10 μm. B(a)P, as the example PAH, was introduced in the model as four different species: three particulate ones in the Aitken, accumulation, and coarse modes and one species in the gas phase. All of these species are treated as inert for the moment; that is, B(a)P does not undergo chemical or photolytic degradation. In particular, for B(a)P this appears to be an acceptable approach because it occurs at temperatures prevailing in middle Europe mainly bound to aerosols. The degradation of particle-bound PAHs is orders of magnitude slower than those of gaseous PAHs (Esteve et al. 2005). To perform dry deposition and scavenging of aerosol-bound B(a)P, the same parameterizations as for organic aerosols in the three different modes are applied. Dry deposition of gaseous B(a)P is carried out by means of the dry deposition velocity of organic acids that is calculated within the modeling system. Also, the gaseous B(a)P is subject to the transport mechanisms, scavenging, and wet and dry deposition simulated by CMAQ (Byun and Ching 1999; Byun and Schere 2006). Further, a new module was introduced into the CMAQ code that calculates the partitioning of PAHs between the gas and the particle phases. Its effect is that the gaseous PAH species is equilibrated with the particulate ones and that the particle-bound PAH is distributed among the three modes. If no particles are present in the treated air parcel, the species will be completely transferred into the gaseous form. It is not intended that fresh aerosols are created in the Aitken mode from gaseous PAH.

a. Aerosol–gas partitioning

The percentage of semivolatile compounds like PAHs that is bound to particles depends on the aerosol mass and surface concentration in the air, the air temperature, the aerosol composition, and the aerosol water content (Pankow and Bidleman 1991). All of this information is available through variables calculated within the CCTM (Byun and Ching 1999). PAHs can be adsorbed to mineral surfaces or elemental carbon, absorbed by organic aerosol, or absorbed by aerosol water (Lohmann and Lammel 2004). For partitioning it is assumed that the concentrations in the gas and the aerosol phases are in equilibrium (Pankow 1987; Pankow and Bidleman 1992). In the approach presented here, there is a direct relationship between adsorption to mineral surface and absorption into aerosol water. Only if the ratio of aerosol water to ammonium sulfate exceeds the solubility of ammonium sulfate, which is considered the major compound in mineral aerosols, is the aerosol treated as wet and absorption into aerosol water takes effect. Accordingly, all inorganic ions are dissolved and no adsorption to inorganic material can take place.

The concentration of the compound that is bound to aerosols in each mode is calculated with

$$a_i = \varphi_i(a_i + g). \tag{1}$$

Here, a_i is the particulate concentration of the compound in mode i ($i = 1, 2, 3$), g is the gaseous concentration, and φ_i is the particulate fraction of the compound in mode i with

$$\varphi_i = \varphi_i^{\mathrm{ad}} + \varphi_i^{\mathrm{oc}} + \varphi_i^{\mathrm{aq}}. \tag{2}$$

Thus, φ_i is the sum of three different φs resulting from adsorption (ad), absorption into organic carbon (oc), and absorption into aerosol water (aq) as will be described below (Cooter and Hutzell 2002).

Because the constraint of mass consistency must hold, g can be replaced by means of the total concentration of the compound c_{tot}:

$$g = c_{\mathrm{tot}} - a_1 - a_2 - a_3. \tag{3}$$

Equations (1) and (3) lead to a system of three linear equations,

$$\begin{bmatrix} 1 & \varphi_1 & \varphi_1 \\ \varphi_2 & 1 & \varphi_2 \\ \varphi_3 & \varphi_3 & 1 \end{bmatrix} \cdot \begin{bmatrix} a_1 \\ a_2 \\ a_3 \end{bmatrix} = c_{\mathrm{tot}} \times \begin{bmatrix} \varphi_1 \\ \varphi_2 \\ \varphi_3 \end{bmatrix}, \tag{4}$$

whose solution yields the particulate concentrations a_i in each mode. The gaseous concentration g can then be calculated with Eq. (3).

b. Aerosol–air partitioning coefficients

The values of φ_i were calculated for each mode independently. Harner and Bidleman (1998) described how the particulate fraction of a compound can be derived from the aerosol–air partitioning coefficient $K_{p,i}$ ($\mathrm{m^3\ \mu g^{-1}}$) that describes the partitioning of a chemical species between the gas and the aerosol phases and the total mass concentration of suspended particles TSP_i ($\mu\mathrm{g\ m^{-3}}$) [Eq. (5)]. This approach was used for calculating φ_i^{oc} and φ_i^{aq} {whereas φ_i^{ad} was calculated directly with the Junge equation [Eq. (10), below]} as follows:

$$\varphi_i^{\mathrm{oc}} = \frac{K_{p,i}^{\mathrm{oc}}\mathrm{TSP}_i}{(K_{p,i}^{\mathrm{oc}}\mathrm{TSP}_i + 1)}, \tag{5}$$

with

$$K_{p,i}^{\mathrm{oc}} = \frac{\dfrac{a_i^{\mathrm{oc}}}{\mathrm{TSP}_i}}{g}. \tag{6}$$

Here $K_{p,i}^{oc}$ is the aerosol–air partitioning coefficient for absorption into the organic carbon and a_i^{oc} is the mass of the compound absorbed by the organic carbon in mode i. The equations for calculating φ_i^{aq} are defined in the same way. In the case of absorption into the organic aerosol phase, Pankow (1994) derived

$$K_{p,i}^{oc} = 10^{-6} f_{OM,i} K_{OA} \frac{M_O \gamma_O}{M_{OM} \gamma_{OM} \rho_O}. \quad (7)$$

The factor 10^{-6} accounts for unit conversions if concentrations of the compound in the gas and the aerosol phase are measured in micrograms per cubic meter, $f_{OM,i}$ is the fraction of organic matter in mode i, K_{OA} is the octanol–air partitioning coefficient, M_O and M_{OM} are the molecular weights of octanol and the organic matter, γ_O and γ_{OM} are the activity coefficients of the compound in octanol and the organic matter phase, and ρ_O is the density of octanol (980 kg m^{-3} at 20°C). Under the assumption that the activity coefficients of the compound in octanol and in the organic aerosol phase are equal and that the organic fraction of the aerosol has the same molecular weight as octanol, this equation simplifies to (Finizio et al. 1991)

$$\log(K_{p,i}^{oc}) = \log(f_{OM,i}) + \log(K_{OA}) - 8.91. \quad (8)$$

In a straightforward way, the partitioning coefficient $K_{p,i}^{aq}$ for absorption into aerosol water can be described by

$$\log(K_{p,i}^{aq}) = \log(f_{W,i}) + \log(K_{WA}) - 9.0, \quad (9)$$

where $f_{W,i}$ is the mass fraction of aerosol water in mode i and K_{WA} is the water–air partitioning coefficient, which is equal to the inverse dimensionless Henry's law constant.

In the case of adsorption, φ_i^{ad} is calculated directly with the Junge equation (Junge 1977) as

$$\varphi_i^{ad} = \frac{cS_i}{p_l + cS_i}. \quad (10)$$

Here, S_i is the surface area concentration of dry aerosol in mode i (cm^{-1}), p_l is the temperature-dependent vapor pressure of the subcooled liquid (Pa), and c is a parameter that characterizes the molecular weight of the sorbate, its concentration in the surface monolayer, and the enthalpies of desorption and evaporation. Harner and Bidleman (1998) reported that for PAHs the proposed value of 17.22 Pa cm is suitable for c. For coarse-mode particles, no such detailed information about the chemical composition of the particles is available. They are assumed not to contain organic matter. Thus, the semivolatile PAHs can only interact with coarse particles through adsorption–desorption processes, and φ_3 is exclusively calculated with Eq. (10).

3. Emissions

As B(a)P emerges from combustion processes, it is emitted primarily adsorbed to fine particles with a diameter between approximately 0.1 and 2 μm (Baek et al. 1991). These particles are represented by the accumulation mode in the CMAQ aerosol routines. However, 0.1% of the B(a)P emissions are put into the Aitken mode, as is done by default with all primary organic aerosols. CMAQ requires hourly emissions (g s^{-1}) for aerosol species placed properly on the model grid domain.

Emission data for B(a)P are very sparse, and the data are connected with large uncertainties. Pacyna et al. (2003) compiled emission inventories of B(a)P projected on the Cooperative Programme for Monitoring and Evaluation of the Long-Range Transmission of Air Pollutants in Europe (EMEP) grid (50 km × 50 km grid in polar stereographic projection); however, from these authors no inventories newer than 1993 are available. Denier Van der Gon et al. (2005) published a technical report on emissions of B(a)P and other POPs for Europe that contains yearly bulk emissions, also projected on the EMEP grid, for 2000. Comparisons of the data for 2000 with those from Pacyna et al. (2003) for 1993 showed that B(a)P emissions have declined substantially since 1993, and so we used the newest available data for our study. They were first interpolated to our CMAQ grid system with the inverse-distance-weighting method under conservation of mass. Because more than 80% of the B(a)P emissions are from residential combustion, a strong dependence of the emissions on season is expected. However, the emission database does not give any information on the temporal assignment of the data, and therefore measurements of B(a)P in ambient air in the vicinity of sources were used to generate weekly scaling factors that were applied to the average emissions in each grid cell. This method resulted in winter emissions that were higher than the annual average by about a factor of 2.5 and summer emissions that were only about one-tenth of the annual average. For weekly and diurnal cycles, emissions from residential combustion follow the same temporal evolution as the carbon monoxide (CO) emissions in the same grid cell and emissions from traffic follow that of nitric oxide. Industrial emissions, as the second important sector, follow weekly but not diurnal cycles.

The CB4 mechanism that comes with the basic CMAQ model was used to calculate concentrations of, for example, the photooxidants; the aerosol mechanism

TABLE 1. Relevant physical–chemical properties of B(a)P at 298 K.

$\log(K_{OA})$	11.1
$\log(K_{WA})$	4.7
$\log(p_l)$	−5.2

(ae4) required some more emission species. Emissions of the trace gases CO, ammonia, nitrogen oxides, sulfur dioxide, and nonmethane volatile organic compounds (NMVOC) as well as emissions of particulate matter with diameter of less than 10 or 2.5 μm (PM10 and PM2.5, respectively), including anthropogenic point and diffuse sources, were provided by the Institute for Energy Economics and the Rational Use of Energy (IER) Stuttgart readily gridded for our 54- and 18-km CMAQ grid as hourly emissions for the entire year of 2000. The NMVOC emissions that were provided in the split of the Regional Acid Deposition Model, version 2, mechanism were converted to the less detailed CB4 mechanism. Although, the reactive species modeled with the CB4 mechanism are not needed for the current B(a)P version of CMAQ, we decided not to simplify the mechanism because all of these reactive species play an important role for the formation of secondary organic aerosols from NMVOCs. Further, they will be needed in our future model versions for which we plan to include chemical degradation of POPs.

4. Boundary and initial conditions

The boundary conditions for the inner domain were derived from simulation results of the outer domain, whereas the boundary conditions of the large grid were set to be near zero. We currently have no exact cognition about the boundary conditions of the outer domain. At the same time, the most significant PAH and particle sources are situated south and east of the model domain while the predominant wind direction is west. Tests showed that boundary conditions for the outer domain do not remarkably influence the B(a)P concentrations in the inner domain. Mean profiles of PM10 were prescribed; all other species were assumed to be zero. This configuration, which minimizes the effects of the chemical mechanism on the number density of the aerosol particles, was chosen to test the transport mechanisms of the model and the ability to represent vertical mixing within the boundary layer.

Initial conditions rapidly lose their influence on the simulated concentrations after significant emissions have been released. However, they have a considerable influence on concentrations during the first simulation day. Thus, the model run was started one day before the time period of interest began. For example, to simulate the concentrations in July the model run was started on 30 June.

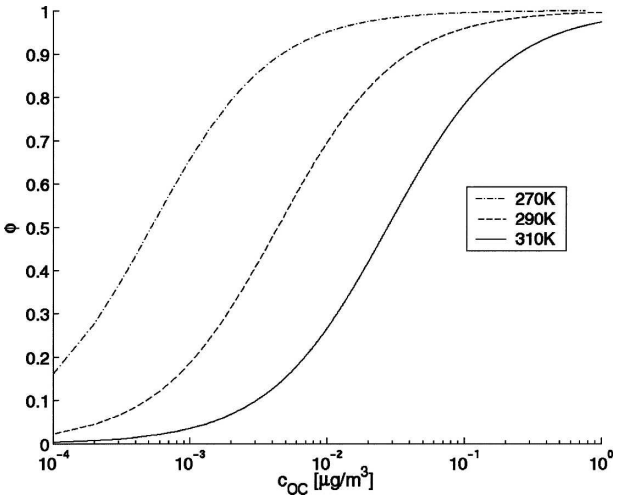

FIG. 1. Dependency of the particulate fraction of B(a)P on temperature and the concentration of particulate organic carbon.

5. Model results and discussion

B(a)P is poorly volatile and highly affinitive to octanol, which represents organic carbon. Thus, the vastly biggest portion of atmospheric B(a)P is bound to aerosols. Among the physical–chemical parameters that determine the aerosol-bound fraction of B(a)P, the octanol–air partitioning coefficient is by far the most important one because $\log(K_{OA})$ is bigger by a factor of approximately 2 than the logarithms of the other physical–chemical parameters (Table 1) (de Maagd et al. 1998). Because of its poor water solubility $\log(K_{AW})$ is smaller than the negative of $\log(p_l)$, and, thus, a high water content of the aerosol retards the adsorption of B(a)P. However, absorption into organic aerosol is so dominant that this effect becomes nearly negligible if organic aerosol is present. Gaseous B(a)P is expected to occur in notable concentrations only if the air temperature is above 280 K, the aerosol concentration is low, and the fraction of organic carbon is extremely small (Fig. 1). Especially in the industrialized regions of Europe and around the big cities, where the sources both for anthropogenic particles and B(a)P are located, the compound can be regarded as entirely aerosol-borne. In the vicinity of the sources by far most of the B(a)P aerosol mass can be found in the accumulation mode in which it is emitted. Some distance away from the source regions, it is also present in the coarse and Aitken modes, depending on the concentration of

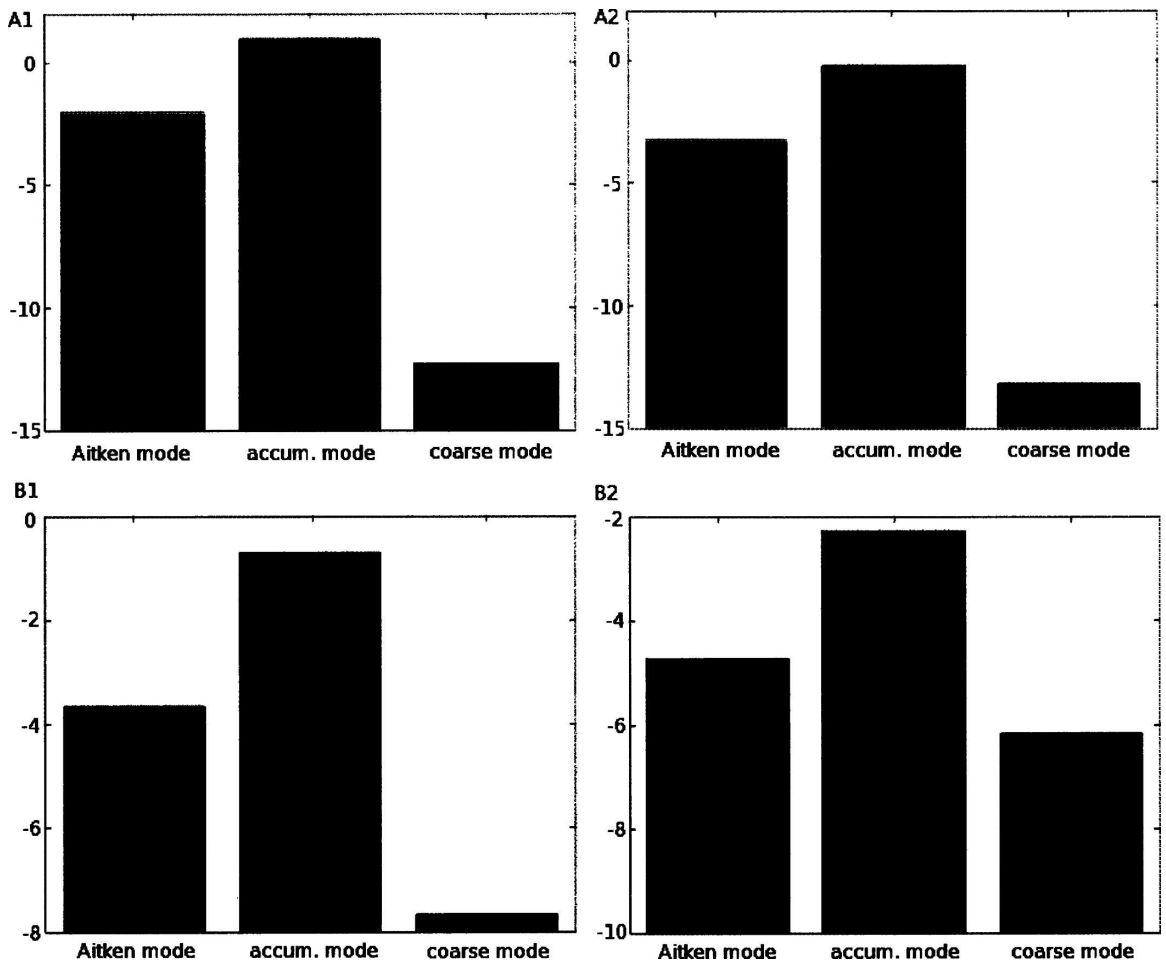

FIG. 2. Distribution of B(a)P mass [log(ng m^{-3})] in aerosols of three different modes in a grid cell (left) within a source region and (right) away from emission sources from simulations for (top) January and (bottom) July.

coarse- and Aitken-mode particles in the air. This can be seen from simulation results and conforms to B(a)P measurements in aerosols of different sizes conducted, for example, by Allen et al. (1996). Allen et al. explain this finding by adsorption–desorption events that happen while aerosol-bound semivolatile substances are transported away from their emission sources. The crucial factor for this behavior in the model is, in fact, the mass concentration and composition of the aerosols in the three different modes and the temperature of the ambient air. Whereas in January virtually all of the B(a)P mass remains in the accumulation mode, in July B(a)P can also be found in the Aitken and coarse modes distant from sources (Fig. 2).

Simulations of concentrations and depositions of B(a)P were carried out for January, April, July, and October 2000. The 4 months were chosen to represent the seasonal variation of the driving meteorological parameters. In January 2000, a typical mix of European winter conditions was present with stable high pressure situations favoring the accumulation of pollutants close to ground, but also with passing low pressure systems leading to a well-mixed boundary layer under windy conditions. The first half of April 2000 was also dominated by passing low pressure systems, but in the end of April central Europe was influenced by warm and dry air masses originating from southeastern Europe. July was not a typical summer month; in central Europe it was colder and wetter than the climatological average. Last, October represented average autumn conditions well although the temperatures in central Europe were very high in the last 10 days of the month. To evaluate the simulation results of the model runs within the outer (54 km $\times$ 54 km) domain, the simulated B(a)P concentrations in 2000 in the lowest model layer have been compared with ground measurements conducted by the EMEP monitoring network (Aas and Hjellbrekke 2003). EMEP data about monthly and yearly

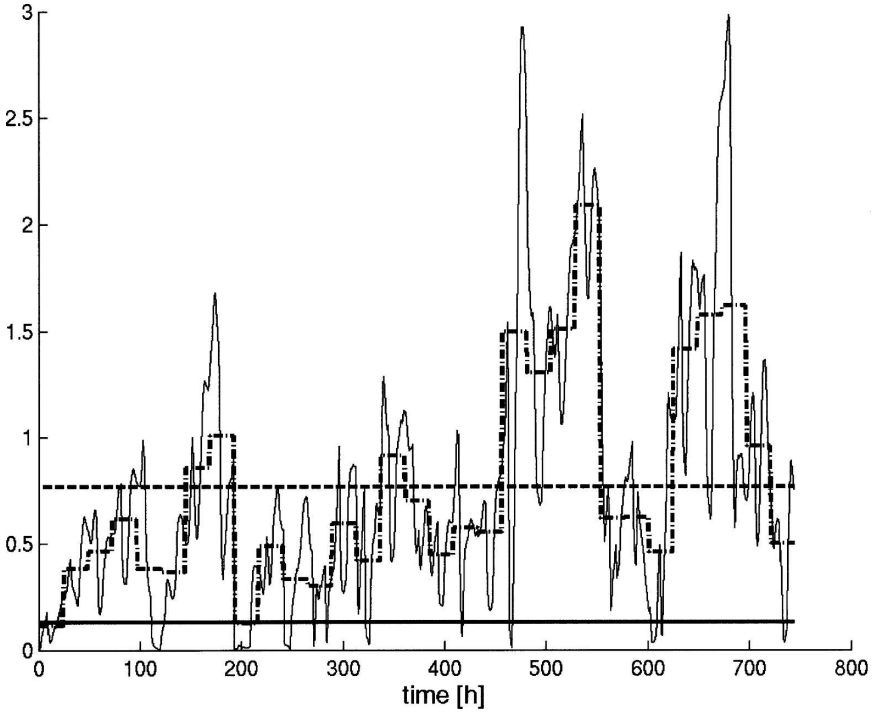

FIG. 3. Comparison of simulated hourly concentrations (ng m^{-3}; thin line) with the measured monthly mean concentration (thick gray line; derived from one daily sample per week) of October 2000 at Kosetice. The dashed line is the monthly mean, and the dash–dotted line displays the daily means calculated from simulations.

mean concentrations of B(a)P are available at four measurement sites—two remote from sources in Sweden (Roervik) and Finland (Pallas), one in the vicinity of Stockholm, Sweden (Aspvreten), and one in a rural area in the Czech Republic (Kosetice). The data were accessible via the Internet (online at http://webdab.emep.int). As an example, in Fig. 3 the measured monthly means of October 2000 at Kosetice are compared with the simulated hourly total B(a)P concentrations of the grid cells in which this EMEP site is located. The simulated concentrations show a high variability. The largest part of the variability is probably caused by daytime/nighttime variations in boundary layer thickness. Other causes are transport mainly by horizontal advection and wet deposition of particles. Dedicated model runs showed that the diurnal emission cycle has only little influence on the variation of concentrations at Kosetice and nearly no influence at remote sites like Pallas. No information about the variability of the measurements is available for the EMEP sites at which different sampling periods applied. At Kosetice, samples were taken at 1 day per week, at Pallas and Roervik 1 week per month was sampled, and at Aspvreten weekly samples were taken. This has to be taken into account when comparing measurements with

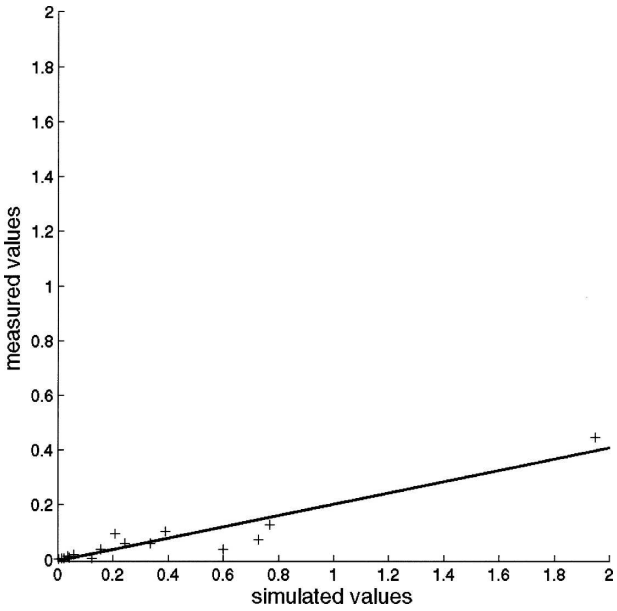

FIG. 4. Scatterplot of simulated monthly mean concentrations of B(a)P (ng m^{-3}) against measured values ($r = 0.94$) at the four EMEP sites.

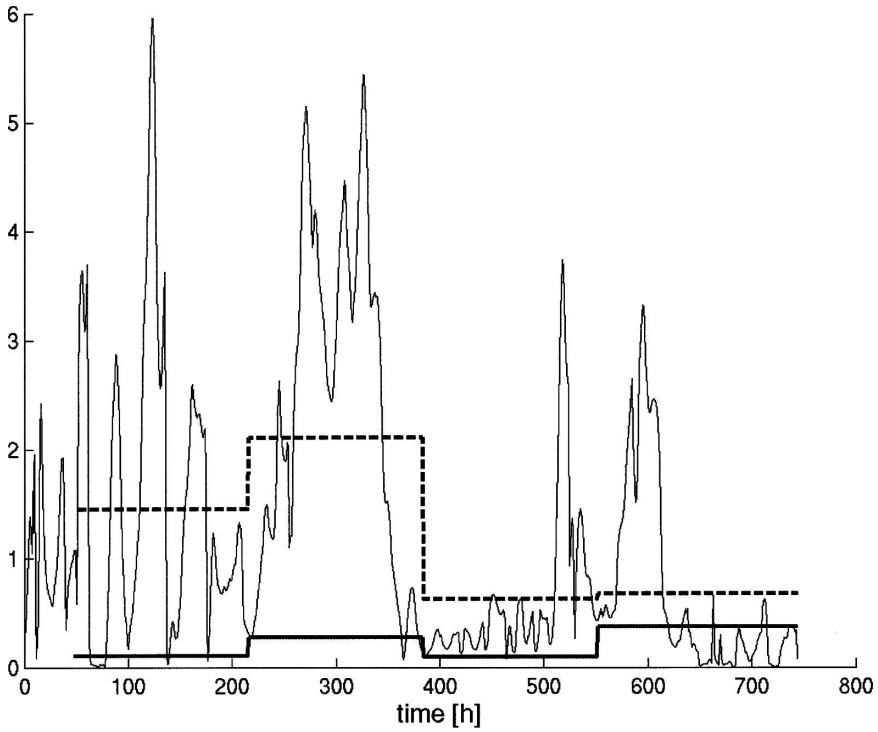

FIG. 5. Comparison of simulated hourly concentrations (ng m^{-3}; thin line) with the measured weekly mean concentration (thick gray line) of April 2000 at Bornhoeved. The dashed line displays weekly means calculated from simulations.

simulated concentrations. Comparing the measured monthly mean values of January, April, July, and October with those calculated from simulations in a scatterplot (Fig. 4) suggests that the correlation between measured and simulated values is good, as also indicated by Pearson's correlation coefficient r of 0.94. However, it can also be seen that the model obviously overestimates the measurements in general. The root-mean-square error of prediction (RMSEP) is 0.477 ng m^{-3}, with measured values ranging from 0.001 to 0.447 ng m^{-3}. On the one hand, a mean error of about 2 times the maximum value would be acceptable with respect to uncertainties both in measurements and emissions. On the other hand, the deviations at low concentrations are much larger. The scatterplot and the mean bias of 421% indicate a significant trend of overestimation. This is not satisfactory and likely is an indication that either the emissions are overestimated or the lack of degradation reactions in the model leads to a nonnegligible overestimation of the atmospheric lifetime of B(a)P. Because the most significant overestimations occur in January where the emissions peak, and not in July when degradation by photolysis or photooxidants is usually most effective, the reason for these discrepancies is rather caused by input data than by the model

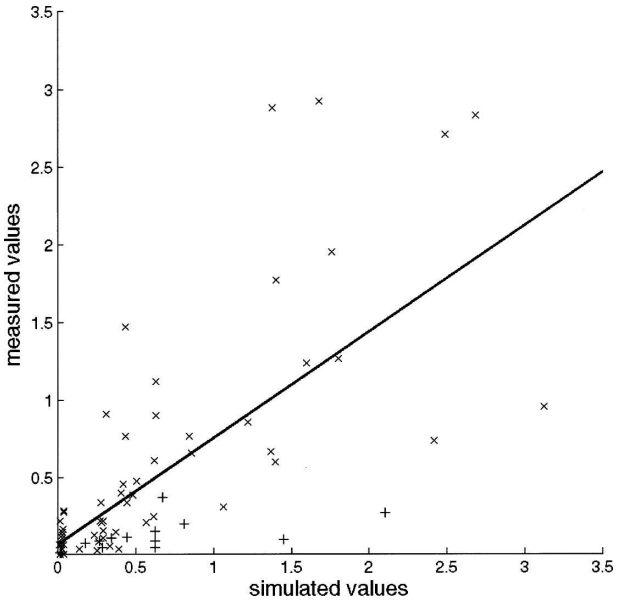

FIG. 6. Scatterplot of simulated mean concentrations of B(a)P (ng m^{-3}) against measured values. The plus signs denote weekly means from Bornhoeved ($r = 0.75$), and the times signs denote 2-day means from Radebeul ($r = 0.58$).

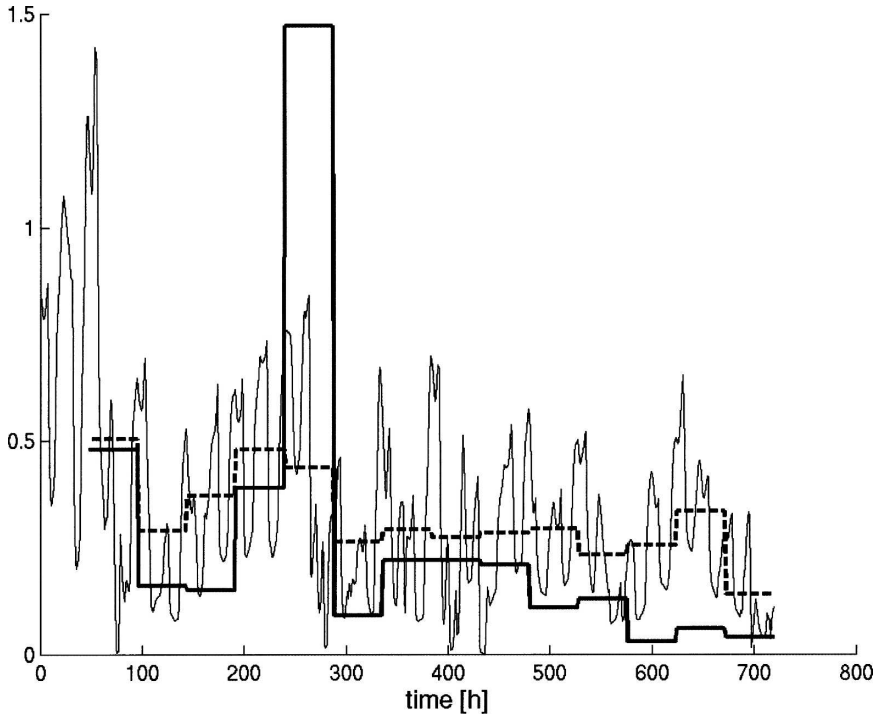

FIG. 7. Comparison of simulated hourly concentrations (ng m^{-3}; thin line) with the measured 2-day mean concentrations (thick gray line) of April 2000 at Radebeul. The dashed line displays 2-day means calculated from simulations.

itself. This is also confirmed by results of the MSCE-POP model that overestimate significantly the yearly mean of 2000 in comparison with measurements (Shatalov et al. 2005). Concentrations of atmospheric constituents near the surface are strongly influenced by vertical mixing within the boundary layer and related exchange across the topping inversion. By comparing modeled temperature and humidity profiles with those from radiosonde measurements, which in the lower atmosphere were not assimilated into the model runs, the model's ability to generate the appropriate boundary layer height was inspected for three representative geographical locations. It was found that the modeled boundary layer depth was matched well, with only a slight tendency to overestimate the actual values. The strength of the inversion at the boundary layer top was often less pronounced in the model fields, however, indicating the possibility of an enhanced exchange of near-surface air to the free troposphere. This mechanism would rather lead to lower than to higher concentrations at the ground and thus cannot explain the deviations between modeled and measured B(a)P concentrations.

Within the nested (18 km × 18 km) domain, two sites of the national German air-quality monitoring program (Ihle and Fritsche 2003) are located. For the first site,

TABLE 2. Comparison of simulated mean concentrations of B(a)P (ng m^{-3}) in 2000 with measured values; single asterisk denotes results from the domain with 54-km grid spacing, and double asterisks denote results from the domain with 18-km spacing.

Station	Lat (°)	Lon (°)	Month	Measured mean	Simulated mean
Kosetice*	49.58	15.08	Jan	0.447	1.947
			Apr	0.059	0.335
			Jul	0.013	0.034
			Oct	0.128	0.767
Aspvreten*	58.80	17.38	Jan	0.072	0.727
			Apr	0.038	0.157
			Jul	0.003	0.015
			Oct	0.094	0.208
Roervik*	57.42	11.93	Jan	0.037	0.599
			Apr	0.060	0.244
			Jul	0.005	0.021
			Oct	0.102	0.390
Pallas*	67.97	24.12	Jan	0.005	0.122
			Apr	0.006	0.042
			Jul	0.001	0.001
			Oct	0.011	0.059
Bornhoeved**	54.09	10.24	Jan	0.211	1.234
			Apr	0.083	0.249
			Jul	0.017	0.015
			Oct	0.132	0.530
Radebeul**	51.12	13.68	Jan	1.492	1.180
			Apr	0.269	0.239
			Jul	0.119	0.018
			Oct	0.673	0.497

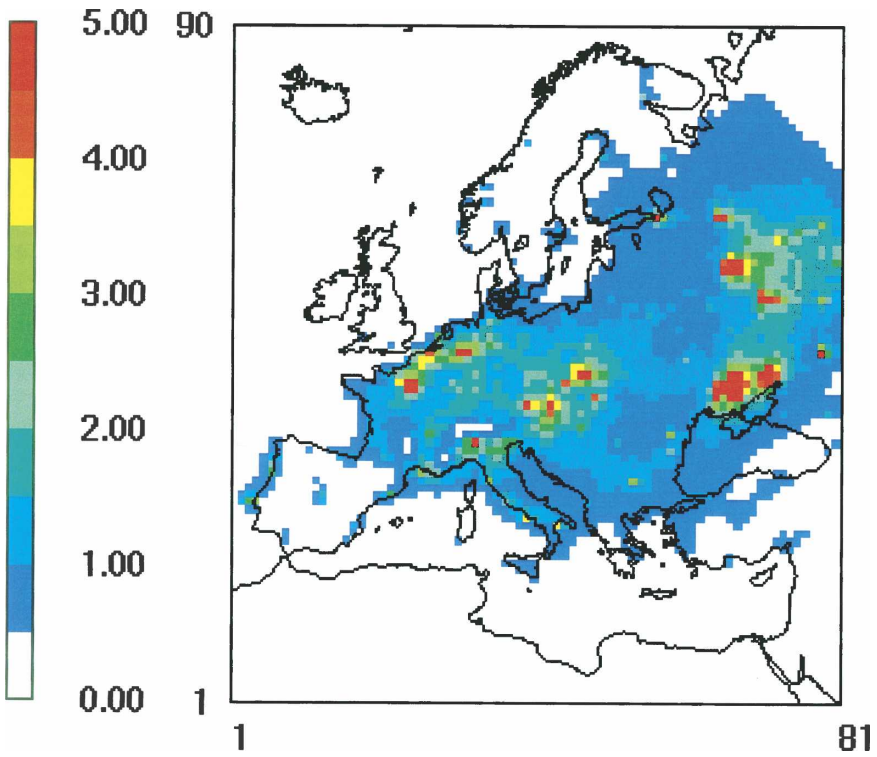

FIG. 8. Simulated monthly mean concentrations of B(a)P (ng m^{-3}) in the lowest model layer in January 2000.

Bornhoeved, situated within a rural area in northern Germany, weekly values are available. These values were compared with weekly means calculated from simulated concentrations (Fig. 5). Like at the EMEP sites, the simulations generally overestimate the measurements (Fig. 6), with a mean bias of 77%. The correlation coefficient r is 0.75, and the RMSEP is 0.598 ng m^{-3}, with measured values varying between 0.017 and 0.374 ng m^{-3}. The second station is located at Radebeul, in a populated area near Dresden. Although the mean bias is only −33% the correlation between measurements and simulations is not very good ($r = 0.58$) and the RMSEP is 0.520 ng m^{-3}, whereas the measurements lie between 0.010 and 2.92 ng m^{-3} (Fig. 7). Emissions in the grid cell to which Radebeul belongs are unevenly distributed, and the city of Dresden, which lies partly in this grid cell, displays a significant source. It is obvious that the measurement station at Radebeul is not representative for the entire grid cell. To cover such small-scale variations, a finer resolution of both the model domain and the emissions map would be required.

Table 2 summarizes the comparisons between model results and ground measurements. The median of the ratio of simulated to measured means is approximately 4. In essence, one has to take into account an error both for simulations and measurements that has been estimated to be up to 50% at low concentrations. Further, point measurements were compared with estimated concentrations averaged over an entire grid cell without taking into account the variability within a grid cell. And, last, a possible reason for the large discrepancy between the monthly mean calculated from measurements and from simulations at Kosetice is that measurements could have taken place on days with low concentration levels and missed days with high concentration levels. Figure 3, at least, indicates this. However, as the main reason for the fact that the modeled concentrations are generally higher than the measured ones, we consider uncertainties in the emissions.

Figure 8 shows the simulated average mean B(a)P concentrations in January 2000 in the bottom layer. The highest concentrations can be found in and around the source regions like the Moscow area or the region between Belgium, the Netherlands, western Germany, and northern France because B(a)P is mainly associated with aerosols and, thus, is deposited to a large extent in the vicinity of the sources. At the same time, however, a part of it is also distributed all over Europe, including areas in which no sources are located, such as the Baltic Sea and southern Finland. The cumulative wet and dry B(a)P depositions into the North Sea for

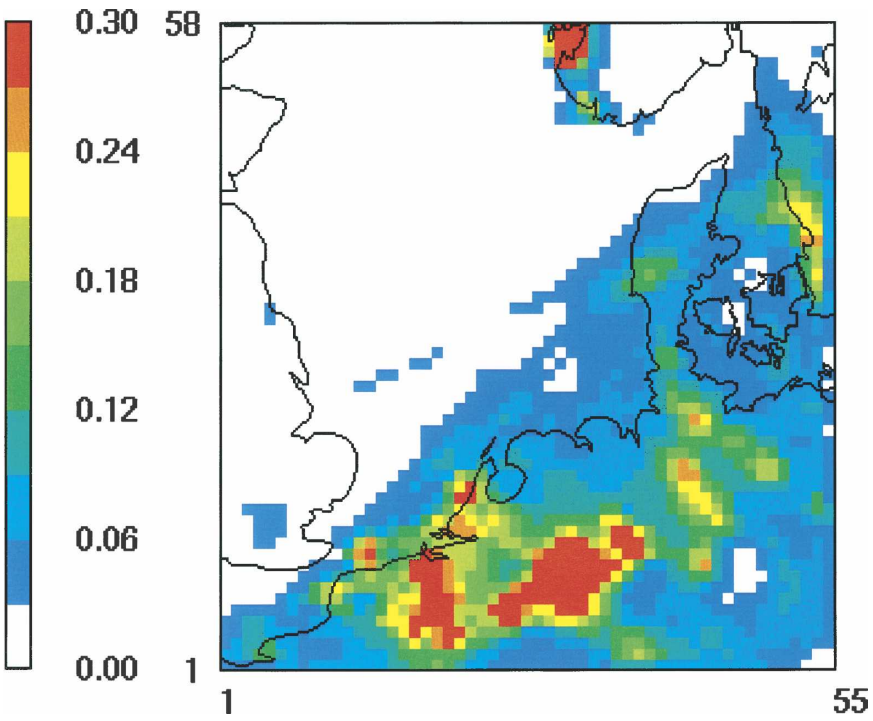

FIG. 9. Simulated cumulative total depositions of B(a)P (g ha^{-1}) within the nested domain in January 2000.

January 2000 can be seen in Fig. 9. Although most of the B(a)P is deposited over land because the emission sources in our model are located exclusively ashore, a nonnegligible amount is also deposited over sea. Significantly higher depositions into the North Sea can be expected if emissions from ship engines and oil platforms are included. The generation of such an emissions database is currently in progress. Especially in the Wadden Sea, where the water is shallow, atmospheric depositions may play an important role for the B(a)P (which represents PAH) budget in the water body and sediments. The quantification of these amounts will be a central application of the CMAQ model for POPs.

6. Conclusions

The evaluation results in this paper suggest that with the here-presented extensions CMAQ is able to simulate fairly well the ambient air concentrations of B(a)P over Europe. This model can be used to assess the transport pathways of B(a)P over Europe at different scales. For further verification of the model performance, long-term runs will be carried out to extend the model validation period to several years. From a model-development point of view and as long as degradation reactions are ignored, changes to apply this version of CMAQ to other POPs are made easily because it is only necessary to insert the respective octanol–air partitioning coefficients, vapor pressure of the subcooled liquid, and Henry's law constant, together with their temperature-dependency functions, into the aerosol–gas partitioning modules. However, for most substances degradation cannot be omitted. Therefore, one of our efforts regarding further development of the model will be focused on introducing degradation of B(a)P and other PAHs in the gas phase, cloud water, and aerosols.

Acknowledgments. NCAR and The Pennsylvania State University are gratefully acknowledged for the use of MM5, and the U.S. EPA is acknowledged for the use of CMAQ. We thank IER Stuttgart and TNO, Appeldoorn, for providing emission data, and EMEP as well as the German Federal Environment Agency are acknowledged for the use of measurement data. A form of this paper was presented during the Community Modeling and Analysis System 2005 annual conference at Chapel Hill, North Carolina.

REFERENCES

Aas, W., and A. Hjellbrekke, 2003: Heavy metals and POP measurements, 2001. Chemical Co-ordinating Centre of EMEP (CCC), Norwegian Institute for Air Research, EMEP/CCC Rep. 1/2003, 114 pp.

Allen, J. O., N. M. Dookeran, K. A. Smith, A. F. Sarofim, K.

Taghizadeh, and A. L. Lafleur, 1996: Measurement of polycyclic aromatic hydrocarbons associated with size-segregated atmospheric aerosols in Massachusetts. *Environ. Sci. Technol.,* **30,** 1023–1031.

Baek, S. O., M. E. Goldstone, P. W. W. Kirk, J. N. Lester, and R. Perry, 1991: Phase distribution and particle size dependency of polycyclic aromatic hydrocarbons in the urban atmosphere. *Chemosphere,* **22,** 503–520.

Baussant, T., S. Sanni, G. Jonsson, A. Skadsheim, and J. F. Borseth, 2001: Bioaccumulation of polycyclic aromatic compounds: 1. Bioconcentration in two marine species and in semipermeable membrane devices during chronic exposure to dispersed crude oil. *Environ. Toxicol. Chem.,* **20,** 1175–1184.

Binkowski, F. S., and U. Shankar, 1995: The regional particulate model. 1. Model description and preliminary results. *J. Geophys. Res.,* **100,** 26 191–26 209.

Byun, D., and J. K. S. Ching, Eds., 1999: Science algorithms of the EPA Models-3 Community Multiscale Air Quality (CMAQ) modeling system. Office of Research and Development, EPA Rep. EPA/600/R-99/030.

——, and K. L. Schere, 2006: Review of the governing equations, computational algorithms, and other components of the Models-3 Community Multiscale Air Quality (CMAQ) modeling system. *Appl. Mech. Rev.,* **59,** 51–77.

Colby, F. R., Jr., 2004: Simulation of the New England sea breeze: The effect of grid spacing. *Wea. Forecasting,* **19,** 277–285.

Cooter, E. J., and W. T. Hutzell, 2002: A regional atmospheric fate and transport model for atrazine. 1. Development and implementation. *Environ. Sci. Technol.,* **36,** 4091–4098.

de Maagd, P. G. J., D. T. E. M. ten Hulscher, H. van den Heuvel, A. Opperhuizen, and D. T. H. M. Sijm, 1998: Physicochemical properties of polycyclic aromatic hydrocarbons: Aqueous solubilities, n-octanol/water partition coefficients, and Henry's law constants. *Environ. Toxicol. Chem.,* **17,** 251–257.

Denier van der Gon, H. A. C., M. van het Bolscher, A. J. H. Visschedijk, and P. Y. J. Zandfeld, 2005: Study of the effectiveness of UNECE Persistent Organic Pollutants Protocol and cost of possible additional measures. Phase I: Estimation of emission reduction resulting from the implementation of the POP Protocol. TNO Rep. B&O-A R 2005/194.

Esteve, W., H. Budzinski, and E. Villenave, 2005: Relative rate constants for the heterogeneous reactions of NO_2 and OH radicals with polycyclic aromatic hydrocarbons adsorbed on carbonaceous particles. Part 2: PAHs adsorbed on diesel particulate exhaust SRM 1650a. *Atmos. Environ.,* **40,** 201–211.

Finizio, A., D. McKay, T. F. Bidleman, and T. Harner, 1991: Octanol–air partition coefficient as a predictor of partitioning of semi-volatile organic chemicals to aerosols. *Atmos. Environ.,* **31,** 2289–2296.

Gery, M. W., G. Z. Whitten, J. P. Killus, and M. C. Dodge, 1989: A photochemical kinetics mechanism for urban and regional scale computer modeling. *J. Geophys. Res.,* **94,** 12 925–12 956.

Grell, G., J. Dudhia, and D. R. Stauffer, 1995: A description of the fifth-generation Penn State/NCAR Mesoscale Model (MM5). NCAR Tech. Note 398, 122 pp.

Gusev, A., E. Mantseva, V. Shatalov, and B. Strukov, 2005: Regional multicompartment model MSCE-POP. Meteorological Synthesizing Centre-East, EMEP/MSC-E Tech. Rep. 5/2005, 79 pp.

Harner, T., and T. F. Bidleman, 1998: Octanol–air partition coefficient for describing particle/gas partitioning of aromatic compounds in urban air. *Environ. Sci. Technol.,* **32,** 1494–1502.

Hong, S. Y., and H. L. Pan, 1996: Nonlocal boundary layer vertical diffusion in a Medium-Range Forecast Model. *Mon. Wea. Rev.,* **124,** 2322–2339.

Ihle, B., and P. Fritsche, 2003: Registration of air pollution by polycyclic aromatic hydrocarbons (PAH) in the Federal Republic of Germany by means of measurement data (in German). Institute for Energy and Environment, Forschungsbericht 20 04 22 66, 178 pp.

Junge, C. E., 1977: Basic considerations about trace constituents in the atmosphere as related to the fate of global pollutants. *Fate of Pollutants in Air and Water Environments, Part I,* I. H. Suffett, Ed., John Wiley and Sons, 7–26.

Kain, J. S., 2004: The Kain–Fritsch convective parameterization: An update. *J. Appl. Meteor.,* **43,** 170–181.

——, and J. M. Fritsch, 1993: Convective parameterization for mesoscale models: The Kain–Fritsch scheme. *The Representation of Cumulus Convection in Numerical Models,* No. 46, *Meteor. Monogr.,* Amer. Meteor. Soc., 165–170.

Lohmann, R., and G. Lammel, 2004: Adsorptive and absorptive contributions to the gas-particle partitioning of polycyclic aromatic hydrocarbons: State of knowledge and recommended parametrization for modeling. *Environ. Sci. Technol.,* **38,** 3793–3803.

MacDonald, R. W., and Coauthors, 2000: Contaminants in the Canadian Arctic: 5 years of progress in understanding sources, occurrence and pathways. *Sci. Tot. Environ.,* **254,** 93–234.

Mumatz, M., and J. George, 1995: Toxicological profile for polycyclic aromatic hydrocarbons. U.S. Department of Health and Human Services, Agency for Toxic Substances and Disease Registry, 458 pp.

Otte, T. L., 1999: Developing meteorological fields. Science Algorithms of the EPA Models-3 Community Multiscale Air Quality Modeling System, U.S. Environmental Protection Agency, Office of Research and Development, EPA/600/R-99/030, 3-1–3-15.

Pacyna, J. M., K. Breivik, J. Münch, and J. Fudala, 2003: European atmospheric emissions of selected persistent organic pollutants, 1970–1995. *Atmos. Environ.,* **37** (Suppl.), 119–131.

Pankow, J. F., 1987: Review and comparative analysis of the theories on partitioning between the gas and aerosol particulate phases in the atmosphere. *Atmos. Environ.,* **22,** 2275–2283.

——, 1994: An absorption model of gas particle partitioning of organic compounds in the atmosphere. *Atmos. Environ.,* **28,** 185–188.

——, and T. F. Bidleman, 1991: Effects of temperature, TSP and percent non-exchangeable material in determining the gas-particle distributions of organic compounds. *Atmos. Environ.,* **25A,** 2241–2249.

——, and ——, 1992: Interdependence of the slopes and intercepts from the log–log correlations of measured gas-particle partitioning and vapour pressure—I. Theory and analysis of available data. *Atmos. Environ.,* **26A,** 1071–1080.

Reisner, J., R. J. Rasmussen, and R. T. Bruintjes, 1998: Explicit forecasting of supercooled liquid water in winter storms using the MM5 mesoscale model. *Quart. J. Roy. Meteor. Soc.,* **124,** 1071–1107.

Shatalov, V., A. Malanitchev, T. Berg, and R. Larsen, 2000: Investigation and assessment of POP transboundary transport

and accumulation in different media. Meteorological Synthesizing Centre-East, EMEP MSC-E Rep. 4/2000, 90 pp.

——, and Coauthors, 2004: POP model intercomparison study. Stage I: Comparison of descriptions of main processes determining POP behaviour in various environmental compartments. Meteorological Synthesizing Centre-East, EMEP MSC-E Rep. 1/2004, 156 pp.

——, and Coauthors, 2005: Modelling of POP contamination in European region: Evaluation of the model performance. Meteorological Synthesizing Centre-East, EMEP MSC-E Rep. 7/2005, 133 pp.

Wania, F., and D. Mackay, 1999: The evolution of mass balance models of persistent organic pollutant fate in the environment. *Environ. Pollut.,* **100,** 223–240.

Wild, S. R., and K. C. Jones, 1995: Polynuclear aromatic hydrocarbons in the United-Kingdom environment—A preliminary source inventory and budget. *Environ. Pollut.,* **88,** 91–108.